The ETDRKP-IF scheme for Allen-Cahn equation with logarithmic Flory-Huggins potential

Xiaoyan Li, Huiping Cai*

***Abstract*—This paper focuses on combining the fourth-order central difference scheme with the fourth-order exponential time-differencing Runge-Kutta (ETDRK4P) method based on Padé rational approximation of matrix exponential, along with dimensional splitting. The resulting ETDRKP-IF scheme is applied to solve the Allen-Cahn equation with logarithmic Flory-Huggins potential. The proposed method achieves fourth-order accuracy in both time and space. Numerical experiments verify the convergence and energy stability of the scheme, providing a reliable method for numerical simulation of the Allen-Cahn equation with logarithmic Flory-Huggins potential.**

***Index Terms*—Allen-Cahn equation, logarithmic potential, exponential time differencing, fourth-order time stepping, dimension splitting.**

I. Introduction

In various phase-field models, the Allen-Cahn (AC) equation with logarithmic Flory-Huggins potential demonstrates significant importance in describing physical processes. Compared to the commonly used quartic polynomial potential, it more accurately reflects real physical phenomena. In this paper, we primarily focus on the following AC equation [1]:

$$\begin{cases} \partial_t u = \varepsilon^2 \Delta u - f(u), (t,x) \in (0,\infty) \times \Omega \\ F(u) = \theta\left[u \ln u + (1-u)\ln(1-u)\right] + \theta_c u(2+u), 0 < u < 1 \\ u|_{t=0} = u^0, \end{cases} \tag{1}$$

where $\Omega \subset \mathbb{R}^2$ is a bounded domain, u is a real-valued function, ε is the mobility coefficient, $F(u)$ denotes the logarithmic Flory-Huggins potential and $f(u) = F'(u)$. θ and θ_c are the absolute and critical temperatures respectively. In this paper, we assume that $\theta_c = 1$. It is well known that the Allen-Cahn equation can be regarded as the L^2-gradient flow of the free energy functional $E(u)$, defined as:

$$E(u) = \int_\Omega \left(\frac{\varepsilon^2}{2} |\nabla u|^2 + F(u) \right) \mathrm{d}x \tag{2}$$

and for smooth solutions of (1), the energy $E(u)$ is non-increasing in time, satisfying:

$$\frac{\mathrm{d}}{\mathrm{d}t} E(u) \le 0. \tag{3}$$

We plot the functions $F(u)$ and $f(u)$ for different values of θ in Fig. 1.

In practice, let g denote the number of uniformly distributed grid points in each spatial direction. The spatial derivatives

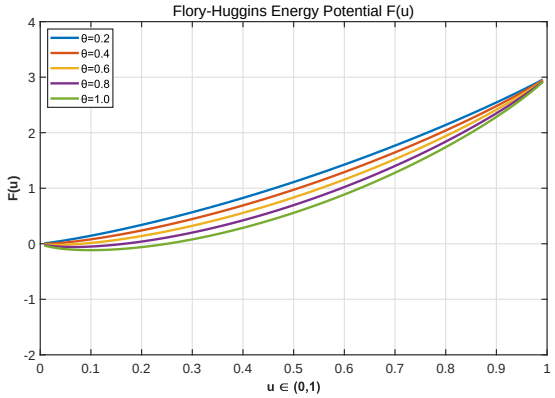

(a) The energy potential $F(u)$

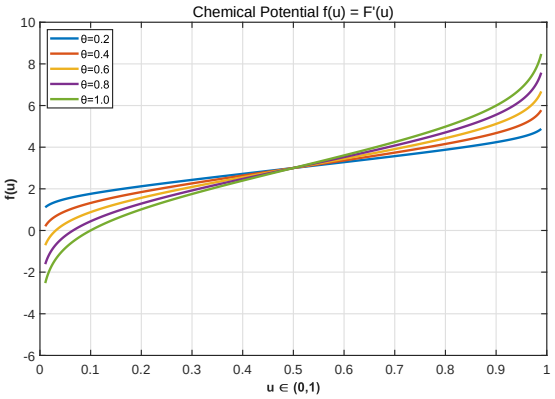

(b) The chemical potential $f(u)$

Fig. 1: The logarithmic Flory-Huggins potential.

in (1) are first discretized on a partition of Ω with g^2 points to obtain a system of ordinary differential equations (ODE):

$$\begin{cases} \frac{dU}{dt} + LU &= N(U(t),t) \\ U(x,0) &= U_0(x), \end{cases}$$

where

$$U = \begin{pmatrix} u_1 \\ \vdots \\ u_g \end{pmatrix},$$

L is the discrete approximation of $-\varepsilon^2\Delta$ and N(U(t),t) is used to approximate all $-f(u)$ on the numerical grid.

From a physical perspective, the logarithmic Flory-Huggins potential is more realistic than the double-well potential. However, its application to the Allen-Cahn equation presents two major difficulties: the logarithmic singularity when the phase variable approaches 0 or 1 and the

Manuscript received April 15, 2025; revised July 18, 2025. This work was supported in part by the NSF of China (No. 11861054), Natural Science Foundation of Guangxi (No. 2020GXNSFAA297223).

Xiaoyan Li is a graduate student of the Guangxi Normal University, Guilin Guangxi 541000, P.R. China (e-mail: lxyan@stu.gxnu.edu.cn).

*Huiping Cai is an associate professor of the College of Mathematics and Statistics in Guangxi Normal University, Guilin 541006, P.R. China (Corresponding author, e-mail: cailp1103@sina.com).

strong nonlinearity of the potential function. Current research primarily addresses these issues through two approaches: At first, constructing specialized numerical schemes. For instance, [2] established a solution framework for the CH/AC system with logarithmic potential and proved properties of the solution but two-dimensional computations require the costly conjugate gradient method. [3] developed an implicit Euler discretization scheme for the one-dimensional case. Secondly, regularization techniques, [4] proposed a stabilized energy decomposition method to prove energy stability, while [5] introduced an efficient algorithm through logarithmic regularization. These contributions provide important references for handling logarithmic potential problems, which arise from the highly nonlinear and stiff nature of the diffusion and reaction terms, as well as the strong nonlinearity of the function $F(u)$. Numerical studies of the Allen-Cahn equation with logarithmic Flory-Huggins potential remain challenging. Additionally, instability may occur if the initial data lacks sufficient smoothness or if the energy parameters are improperly set or incompatible with boundary values. We adopt the dimensional splitting idea from [6], [7] and [8] and employ the exponential time-differencing Runge-Kutta (ETD-RK) scheme from [9] to approximate the exact solution of the ODE system.

Traditional ETD-RK scheme suffers from computational efficiency issues due to matrix exponential operations. To address this, researchers have proposed various improvements. Among them, the ETDRK-Padé scheme in [10], [11], [12] and [13] significantly improves computational speed by using Padé rational approximations for matrix exponentials, with both second-order and fourth-order versions currently available. Additionally, the ETD-RDP scheme in [14], which employs real distinct pole (RDP) rational functions, can further optimize computational performance. To enhance the efficiency of second-order ETD-RK scheme for multidimensional problems, references [15] and [16] proposed improved schemes based on dimensional splitting techniques combined with Padé(1,1) approximation and RDP rational functions, respectively. Recently, the ETDRK4P22-IF scheme proposed in [17] is a more efficient fourth-order exponential time differencing method. It combines dimensional splitting techniques with Padé(2,2) rational approximation for matrix exponentials to solve reaction-diffusion equations, achieving fourth-order accuracy in these systems.

In this paper, we employ the ETDRKP-IF scheme to solve the Allen-Cahn (AC) equation with logarithmic Flory-Huggins potential. Compared to the strongly split method with logarithmic Flory-Huggins potential for solving the AC equation in [1], our approach significantly improves error accuracy and increases the convergence order from second-order to fourth-order. Last but not least, through numerical experiments, we verify the fourth-order accuracy, effectiveness, and energy stability of the ETDRKP-IF scheme for solving the AC equation.

The remainder of this paper is organized as follows. Section 2 presents the spatial discretization. Section 3 introduces the ETDRKP-IF scheme derived from Padé rational approximation of matrix exponentials. Section 4 presents numerical experiments. Finally, conclusions are given in Section 5.

II. Discretization in space

Now construct the two-dimensional Laplacian operator using the Kronecker product. In two dimensional (2D) case, Let $L = L_1 + L_2$ be the matrix approximation of Laplacian with L_1 and L_2 as the matrix approximations of ∂_{xx} and ∂_{yy} respectively in 2D. Let L_p serves as the matrix approximation of the second-order partial derivative in one dimension, and I is an p-dimensional identity matrix. Then $L_1 = L_p \otimes I_p$ and Ł$_2 = I_p \otimes L_p$. Since references [12] and [13] have proved that the matrices L_1 and L_2 commute, so we can perform dimensional splitting. By decomposing L into L_1 and L_2, we reduce the number of non-zero diagonals, thereby accelerating the solution of the linear system.

Similarly, in three dimensional (3D) case we have

$$L = L_1 + L_2 + L_3 \text{ with}$$
$$L_1 = I_p \otimes I_p \otimes L_p, L_2 = I_p \otimes L_p \otimes I_p \text{ and } L_3 = L_p \otimes I_p \otimes I_p.$$

Next, discretize the Laplacian $\Delta = \partial_{xx} + \partial_{yy}$ on the domain $[c,d] \times [c,d]$. A uniform mesh is constructed by partitioning each spatial direction into g grid points with mesh size $h = \frac{d-c}{g-1}$ with $g \geq 5$. Then we set $x_j = c + jh$ with $j = 0, 1, \ldots, g-1$. The second-order partial derivative of a function $v(x,t)$ with respect to x at x_j can be discretized using the fourth-order central difference scheme

$$\partial_{xx} V|_{x_j} = \frac{1}{12h^2}(-V_{j-2} + 16V_{j-1} - 30V_j + 16V_{j+1} - V_{j+2}) + O(h^4), \tag{4}$$

where $j = 2, 3, \ldots, g-3$, with $V_j \approx v(x_j, t)$.

When performing numerical calculations using central difference scheme, we need to consider the treatment of boundary values for both homogeneous Dirichlet and Neumann boundary conditions. For homogeneous Dirichlet boundary condition, we employ fourth-order Lagrange interpolation polynomials to extrapolate and approximate the values at boundary points. For homogeneous Neumann boundary conditions, we introduce symmetric assumptions about virtual node values to approximate the values at boundary points. These methods utilize high-order interpolation and symmetry treatment, effectively ensuring the accuracy and stability of numerical computations near boundaries.

III. Discretization in time

In two dimensional, we present the dimensionally split form ETDRKP-IF of the fourth-order exponential time differencing Runge-Kutta (ETD-RK) scheme using Padé $(2,2)$ rational function approximation ([18],pp. 436]) to solve semilinear ordinary differential equation (ODE) systems.

$$\begin{aligned}
U_{n+1} &= e^{-kL}U_n + P_1(kL)N(U_n, t_n) \\
&\quad + 2P_2(kL)\Big[N\left(a_n, t_n + \tfrac{k}{2}\right) + N\left(b_n, t_n + \tfrac{k}{2}\right)\Big] \\
&\quad + P_3(kL)N(c_n, t_n + k), \\
a_n &= e^{-\frac{k}{2}L}U_n + \tilde{P}(kL)N(U_n, t_n), \\
b_n &= e^{-\frac{k}{2}L}U_n + \tilde{P}(kL)N\left(a_n, t_n + \tfrac{k}{2}\right), \\
c_n &= e^{-\frac{k}{2}L}a_n + \tilde{P}(kL)\Big[2N\left(b_n, t_n + \tfrac{k}{2}\right) - N(U_n, t_n)\Big],
\end{aligned} \tag{5}$$

where

$$\begin{aligned}
P_1(kL) &= \tfrac{1}{k^2}(-L)^{-3}\Big[-4I + kL + e^{-kL}(4I + 3kL + k^2L^2)\Big],\\
P_2(kL) &= \tfrac{1}{k^2}(-L)^{-3}\Big[2I - kL - e^{-kL}(2I + kL)\Big],\\
P_3(kL) &= \tfrac{1}{k^2}(-L)^{-3}\Big[-4I + 3kL - k^2L^2 + e^{-kL}(4I + kL)\Big],\\
\tilde{P}(kL) &= -L^{-1}(e^{-\frac{k}{2}L} - I).
\end{aligned} \tag{6}$$

Next, we incorporate the dimensional splitting technique into this scheme to obtain the fully discrete fourth-order exponential time differencing Runge-Kutta (ETD-RK) scheme in split form like in [17]. The ETDRK-IF scheme is given as follows:

$$\begin{aligned}
U_{n+1} &= e^{-kL_1}e^{-kL_2}U_n + P_1(kL_2)e^{-kL_1}N(U_n, t_n)\\
&\quad + 2P_2(kL_2)e^{-\frac{k}{2}L_1}G\left(\bar{a}_n, \bar{b}_n, t_n + \frac{k}{2}\right)\\
&\quad + P_3(kL_2)N(\bar{c}_n, t_n + k),\\
\bar{a}_n &= e^{-\frac{k}{2}L_2}e^{-\frac{k}{2}L_1}U_n + \tilde{P}(kL_2)e^{-\frac{k}{2}L_1}N(U_n, t_n),\\
\bar{b}_n &= e^{-\frac{k}{2}L_2}e^{-\frac{k}{2}L_1}U_n + \tilde{P}(kL_2)N\left(\bar{a}_n, t_n + \frac{k}{2}\right),\\
\bar{c}_n &= e^{-\frac{k}{2}L_2}e^{-\frac{k}{2}L_1}a_n + \tilde{P}(kL_2)\Big[2e^{-\frac{k}{2}L_1}N\left(\bar{b}_n, t_n + \frac{k}{2}\right)\\
&\quad - e^{-kL_1}N(U_n, t_n)\Big],
\end{aligned} \tag{7}$$

where

$$G\left(\bar{a}_n, \bar{b}_n, t_n + \frac{k}{2}\right) = N\left(\bar{a}_n, t_n + \frac{k}{2}\right) + N\left(\bar{b}_n, t_n + \frac{k}{2}\right).$$

Since both the ETD-RK scheme and ETDRK-IF scheme involve high powers of matrix inversions and matrix exponential computations, they result in prohibitively high computational costs. In some cases (e.g., with coefficient matrices derived from partial differential equations with Neumann boundary conditions), these computations may even become infeasible. To address these challenges, [17] introduced Padé $(2,2)$ rational functions to approximate the matrix exponentials in equation (7).

We denote the Padé $(2,2)$ approximations of e^{-kL} and $e^{-\frac{k}{2}L}$ by $R_{2,2}(kL)$ and $\tilde{R}_{2,2}(kL)$, respectively, thus obtaining the representations:

$$\begin{aligned}
e^{-kL} &\approx R_{2,2}(kL)\\
&= (12I - 6kL + k^2L^2)(12I + 6kL + k^2L^2)^{-1},
\end{aligned} \tag{8}$$

$$\begin{aligned}
e^{-\frac{k}{2}L} &\approx \tilde{R}_{2,2}(kL)\\
&= (48I - 12kL + k^2L^2)(48I + 12kL + k^2L^2)^{-1}.
\end{aligned} \tag{9}$$

By substituting these approximations into both the ETD-RK and ETDRK-IF schemes, we derive the following fully discrete ETDRKP scheme and ETDRKP-IF scheme:

$$\begin{aligned}
a_n &= \tilde{R}_{2,2}(kL)U_n + \tilde{P}(kL)N(U_n, t_n),\\
b_n &= \tilde{R}_{2,2}(kL)U_n + \tilde{P}(kL)N\left(a_n, t_n + \tfrac{k}{2}\right),\\
c_n &= \tilde{R}_{2,2}(kL)a_n + \tilde{P}(kA)\Big[2N\left(b_n, t_n + \tfrac{k}{2}\right) - N(U_n, t_n)\Big],\\
U_{n+1} &= R_{2,2}(kL)U_n + P_1(kL)N(U_n, t_n)\\
&\quad + 2P_2(kL)G\left(a_n, b_n, t_n + \tfrac{k}{2}\right)\\
&\quad + P_3(kL)N(c_n, t_n + k).
\end{aligned} \tag{10}$$

and

$$\begin{aligned}
\bar{a}_n &= \tilde{R}_{2,2}(kL_2)\tilde{R}_{2,2}(kL_1)U_n\\
&\quad + \tilde{P}(kL_2)\tilde{R}_{2,2}(kL_1)N(U_n, t_n).
\end{aligned} \tag{11}$$

$$\begin{aligned}
\bar{b}_n &= \tilde{R}_{2,2}(kL_2)\tilde{R}_{2,2}(kL_1)U_n\\
&\quad + \tilde{P}(kL_2)N\left(\bar{a}_n, t_n + \tfrac{k}{2}\right).
\end{aligned} \tag{12}$$

$$\begin{aligned}
\bar{c}_n &= \tilde{R}_{2,2}(kL_2)\tilde{R}_{2,2}(kL_1)\bar{a}_n\\
&\quad + \tilde{P}(kL_2)\Big[2\tilde{R}_{2,2}(kL_1)N\left(\bar{b}_n, t_n + \tfrac{k}{2}\right)\\
&\quad - R_{2,2}(kL_1)N(U_n, t_n)\Big].
\end{aligned} \tag{13}$$

$$\begin{aligned}
U_{n+1} &= R_{2,2}(kL_1)R_{2,2}(kL_2)U_n\\
&\quad + P_1(kL_2)R_{2,2}(kL_1)N(U_n, t_n)\\
&\quad + 2P_2(kL_2)\tilde{R}_{2,2}(kL_1)G\left(\bar{a}_n, \bar{b}_n, t_n + \tfrac{k}{2}\right)\\
&\quad + P_3(kL_2)N(\bar{c}_n, t_n + k).
\end{aligned} \tag{14}$$

IV. Numerical experiment

In this section in order to demmonstrate the accuracy and energy stability, we conducted numerical experiments on the computational domain $\Omega = [0,1]^2$ with periodic boundary conditions.

Example 1. The initial value is given by

$$u = \begin{cases} 10^{-5}, & |x| \le 0.35 \text{ and } |y| \le 0.35,\\ 1 - 10^{-5}, & \text{otherwise.} \end{cases}$$

We set the spatial discretization is fixed at $h = 0.009817$, while the physical parameters are chosen as $\theta = 0.8$, $\theta_c = 1$, $\varepsilon = 0.01$ and use the time step sizes $\tau = 0.05, 0.025, 0.0125, 0.00625$. In TABLE I, we give the temporal convergence of the numerical solution u. It can be easily observed that the proposed scheme is of fourth-order accuracy for the AC equation. The Fig. 2 confirms the numerical accuracy and computational efficiency of the ETDRKP-IF scheme: Fig. 2 (a) illustrates the relationship between time step size and numerical error, showing that the error decreases significantly as the time step reduces; Fig. 2 (b) compares the error versus CPU time, confirming the superior computational efficiency of this scheme.

TABLE I: Results for ETDRKP-IF to solve AC equation.

τ	h	error	conv	time
0.050000	0.009817	2.3086e-04	0.00	1.39122
0.025000	0.009817	1.5278e-05	3.92	2.81636
0.012500	0.009817	9.5036e-07	4.01	5.40061
0.006250	0.009817	6.2458e-08	3.93	10.94418

Example 2. The initial data is given by

$$u = \text{rand}(x, y).$$

The random data are set between 0 and 1, with parameters $h = \frac{1}{80}$, $\theta = 0.8$, $\theta_c = 1$, $\varepsilon = 0.01$, $T = 500$(final time) and $\tau = 0.01$. We then plot the evolution of the corresponding discrete energy in Fig. 3, the graph shows that the discrete energy decay is most evident when $0 \le t \le 8$ and the discrete energy strictly decreases and eventually stabilizes over time. Additionally, Fig. 4 simulates the dynamic evolution of the phase variable u at $t = 0$, 20, 100, 150, 200, 500. We

can clearly observe the phase separation process, which eventually reaches a steady state.

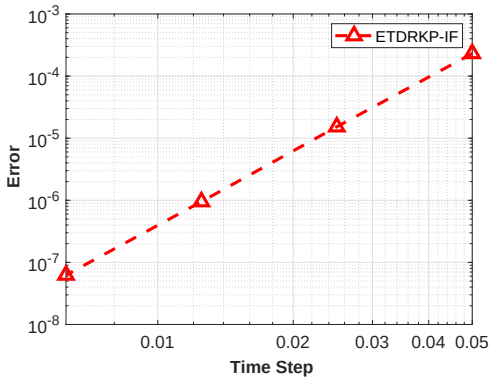

(a) Convergence of ETDRKP-IF

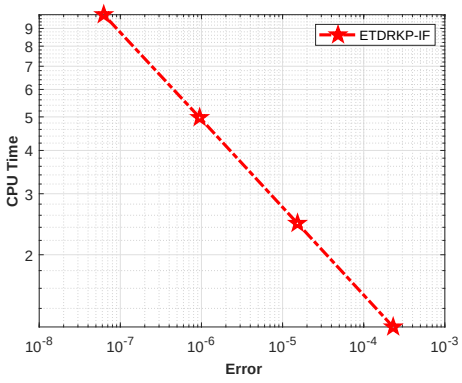

(b) Computational efficiency of ETDRKP-IF

Fig. 2: Convergence and efficiency for ETDRKP-IF.

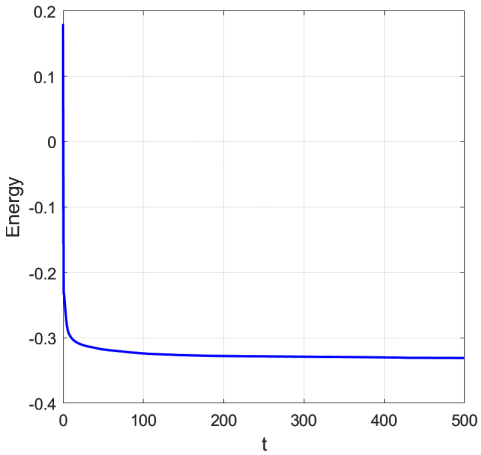

Fig. 3: The curves of the discrete energy.

Example 3. Firstly, the initial data is given by

$$u = \tanh\left(\frac{|x+y|+|x-y|-0.4}{\sqrt{2}\varepsilon}\right).$$

In this example, the evolution of a square bubble is simulated with parameters $T = 120$, $h = \frac{1}{120}$, $\varepsilon = 0.01$,$\theta = 0.8$, $\theta_c = 1$ and $\tau = 0.01$. Then, the dynamic evolution of the phase variable u at $t = 0, 20, 50, 60, 80, 120$ is simulated in Fig. 5. We can clearly observe that the square bubble evolves into a stable circular bubble over time.

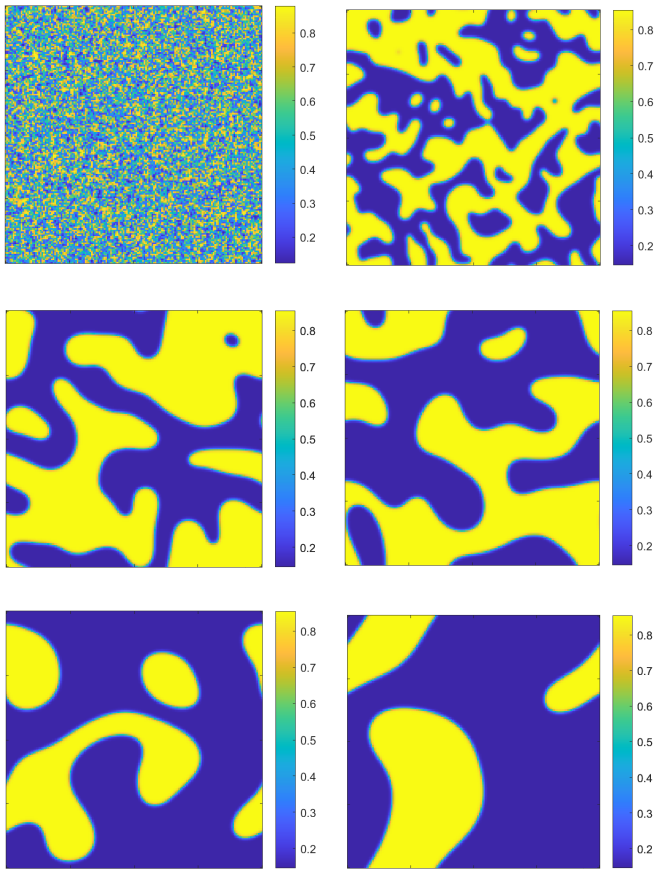

Fig. 4: The dynamical evolutionof the phase variable u at t=0,20,100,150,200,500.

V. Conclusion

This paper employs a fourth-order exponential time-differencing Runge-Kutta scheme with Padé approximation and dimensional splitting (ETDRKP-IF) for solving the Allen-Cahn equation with logarithmic Flory-Huggins potential. The method significantly improves computational efficiency for solving the Allen-Cahn equation with logarithmic Flory-Huggins potential. Theoretical analysis and numerical experiments demonstrate that the ETDRKP-IF scheme achieves fourth-order accuracy in both time and space dimensions, shows marked improvement in computational efficiency compared to traditional strong-splitting methods, while strictly maintaining energy dissipation properties. Notably, the method effectively overcomes the singularity issues of the logarithmic potential when the phase variable approaches 0 or 1, and ensures computational stability through high-order boundary treatment techniques. Numerical simulations clearly reproduce phase separation dynamics, including pattern formation from random initial conditions and the evolution of square bubbles to circular equilibrium states. These results provide reliable tools for numerical studies of complex phase-field systems. Future work will focus on extending this method to three-dimensional problems and further enhancing its ability to handle strong nonlinear terms and complex boundary conditions.

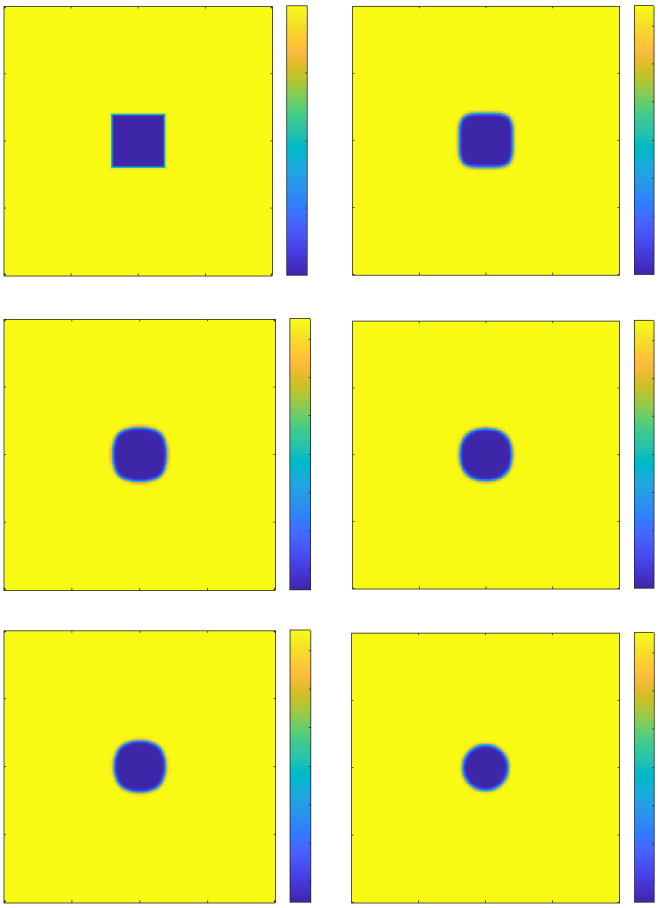

Fig. 5: The dynamical evolutionof the phase variable u at t=0,20,50,60,80,120.

References

[1] C. Wu, X. Feng, Y. He, and L. Qian, A second-order Strang splitting scheme with exponential integrating factor for the Allen-Cahn equation with logarithmic Flory-Huggins potential, *Commun. Nonlinear Sci. Numer. Simul.*, vol. 117, pp. 106983, 2023.

[2] M. Gokielit, L. Marcinkowskii, Discrete approximation of the Cahn-Hilliard/Allen-Cahn system with logarithmic entropy, *Japan J. Ind. Appl. Math*, vol. 20, pp. 321–351, 2003.

[3] M. Copetti, C. Elliott, Numerical analysis of the Cahn-Hilliard equation with a logarithmic free energy, *Numer. Math*, vol. 63, no. 1, pp. 39–65, 1992.

[4] X. Wang, J. Kou, J. Cai, Stabilized energy factorization approach for Allen-Cahn equation with logarithmic Flory-Huggins potential, *J. Sci. Comput*, vol. 82, no. 2, pp. 25, 2020.

[5] D. Jeong, S. Lee, J. Kim, An efficient numerical method for evolving microstructures with strong elastic inhomogeneity, *Model. Simul. Mater. Sci. Eng*, vol. 23, no. 4, pp. 045007, 2015.

[6] E. O. Asante-Asamani, A. Q. M. Khaliq, B. A. Wade, A real distinct poles exponential time differencing scheme for reaction-diffusion systems, *J. Comput. Appl. Math*, vol. 299, pp. 24–34, 2016.

[7] E. O. Asante-Asamani, B. A. Wade, A dimensional splitting of ETD schemes for reaction-diffusion systems, *Commun. Comput. Phys*, vol. 19, no. 5, pp. 1343–1356, 2016.

[8] E. O. Asante-Asamani, A. Kleefeld, B. A. Wade, A second-order exponential time differencing scheme for non-linear reaction-diffusion systems with dimensional splitting, *J. Comput. Phys*, vol. 415, p-p. 109490, 2020.

[9] X. Yang, J. Zhao, On linear and unconditionally energy stable algorithms for variable mobility Cahn-Hilliard type equation with logarithmic Flory-Huggins potential, *Commun. Comput. Phys*, vol. 25, no. 3, pp. 703–728, 2019.

[10] B. Kleefeld, A. Q. M. Khaliq, B. A. Wade, An ETD Crank-Nicolson method for reaction-diffusion systems, *Numer. Methods Partial Differ. Equ*, vol. 28, pp. 1309–1335, 2012.

[11] M. Yousuf, A. Q. M. Khaliq, B. Kleefeld, The numerical approximation of nonlinear Black-Scholes model for exotic path-dependent American options with transaction cost, *Int. J. Comput. Math*, vol. 89, no. 9, pp. 1239–1254, 2012.

[12] M. Yousuf, Efficient L-stable method for parabolic problems with application to pricing American options under stochastic volatility, *Appl. Math. Comput*, vol. 213, no. 1, pp. 121–136, 2009.

[13] A. Q. M. Khaliq, J. Martin-Vaquero, B. A. Wade, M. Yousuf, Smoothing schemes for reaction-diffusion systems with nonsmooth data, *J. Comput. Appl. Math*, vol. 223, no. 1, pp. 374–386, 2009.

[14] E. O. Asante-Asamani, A. Q. M. Khaliq, B. A. Wade, A real distinct poles exponential time differencing scheme for reaction-diffusion systems, *J. Comput. Appl. Math*, vol. 299, pp. 24–34, 2016.

[15] E. O. Asante-Asamani, B. A. Wade, A dimensional splitting of ETD schemes for reaction-diffusion systems, *Commun. Comput. Phys*, vol. 19, no. 5, pp. 1343–1356, 2016.

[16] E. O. Asante-Asamani, A. Kleefeld, B. A. Wade, A second-order exponential time differencing scheme for non-linear reaction-diffusion systems with dimensional splitting, *J. Comput. Phys*, vol. 415, p-p. 109490, 2020.

[17] E. O. Asante-Asamani, A. Kleefeld, and B. A. Wade, A fourth-order exponential time differencing scheme with dimensional splitting for non-linear reaction-diffusion systems, *J. Comput. Appl. Math*, 2025.

[18] S. M. Cox, P. C. Matthews, Exponential time differencing for stiff systems, *J. Comput. Phys*, vol. 176, pp. 430–455, 2002.

[19] J. H. Mathews, K. D. Fink, et al., *Numerical Methods Using MATLAB*, 4th ed., vol. 4, Pearson Prentice Hall, 2004.